Rotation of the Pinning Direction in the Exchange Bias Training Effect in Polycrystalline NiFe/FeMn Bilayers

X. P. Qiu, D. Z. Yang, and S. M. Zhou

Applied Surface Physics Laboratory (State Key Laboratory) and The State Key Lab for Advanced Photonic Materials Devices and Department of Physics, Fudan University, Shanghai 200433, China

R. Chantrell, K. O'Grady, and U. Nowak

Physics Department, The University of York, York, YO10 5 DD, United Kingdom

J. Du and X. J. Bai

National Laboratory of Solid State Microstructures, Nanjing University, Nanjing 210093, China

L. Sun

Department of Mechanical Engineering, University of Houston, Houston, Texas 77204, USA

(Received 22 January 2008; published 3 October 2008)

For polycrystalline NiFe/FeMn bilayers, we have observed and quantified the rotation of the pinning direction in the exchange bias training and recovery effects. During consecutive hysteresis loops, the rotation of the pinning direction strongly depends on the magnetization reversal mechanism of the ferromagnet layer. The interfacial uncompensated magnetic moment of antiferromagnetic grains may be irreversibly switched and rotated when the magnetization reversal process of the ferromagnet layer is accompanied by domain wall motion and domain rotation, respectively.

DOI: 10.1103/PhysRevLett.101.147207 PACS numbers: 75.30.Gw, 75.30.Et, 75.60.Jk

Exchange bias (EB) in ferromagnet (FM)/antiferromagnet (AFM) bilayers has attracted much attention because of its importance in developing magneto-electronic devices [1,2]. In the EB training effect, the exchange field H_E and the coercivity H_C decrease during consecutive measurements of hysteresis loops [3]. Since its first discovery, the training effect has been extensively studied, both experimentally and theoretically [3–11]. Very recently, the training effect and the hysteresis loop asymmetry have been found to be correlated to each other after the first magnetization reversal of the FM layer [9]. To explain the training effect, various theoretical models have been proposed [3,4,6,7]. In an early approach [3], AFM spins are assumed to undergo thermally activated transitions during the magnetization reversal process of the FM layer. To account for the athermal training effect, characterized by a large irreversible change between the first and second hysteresis loops which occurs even at low temperatures, AFM spins are proposed to spin-flop between easy axes [6]. Currently, it is generally believed that the AFM spins play a crucial role in the EB training effect [12,13]. However, a complete picture of the motion of AFM spins behind the phenomenon still remains unclear.

The lack of detailed understanding of the motion of the AFM spins arises for a number of reasons. Principally, it is difficult to probe experimentally the rearrangement of AFM spins during the magnetization reversal process of the FM layer due to the zero net magnetization of the AFM layer. Secondly, in the studies of the training effect, hysteresis loops are often measured only along the cooling field [3,9]. In particular, most attention has been focused on the reduction in magnitude of H_E and H_C with the number of cycles n. The orientation change of the pinning direction (PD) has been ignored. Actually, the PD in FM/AFM bilayers can be directly measured using reversible anisotropic magnetoresistance to demonstrate the motion of the AFM spins [14,15]. In this Letter, we have for the first time directly observed and quantified the PD rotation in the EB training effect. Both the orientation change of the PD and the behavior of the AFM spins are demonstrated to depend on the magnetization reversal mechanism of the FM layer.

A bilayer of $Ni_{80}Fe_{20}$(NiFe)(3 nm)/$Fe_{50}Mn_{50}$(FeMn) was sputtered on a 1 cm $\times$ 5 cm glass substrate at ambient temperature. With a wedge shape across the distance of 5 cm, the FeMn layer thickness t_{AFM} is a linear function of the sampling location. A uniform bilayer of NiFe(3 nm)/FeMn (2.4 nm) was also prepared. A 15 nm Cu buffer layer was used to stimulate the fcc (111) preferred growth of FeMn and to enhance EB [16]. The EB was established by a magnetic field applied in the film plane during deposition. Detailed fabrication procedures were given elsewhere [17].

X-ray diffraction shows that the constituent layers are polycrystalline with fcc (111) and fcc (200) peaks. Before magnetic measurements, the large specimen was cut into small pieces along the wedge direction. With a vector vibrating sample magnetometer (VVSM), m_x and m_y were measured simultaneously, as components of the magnetic moment parallel and perpendicular to the in-plane external magnetic field H. The two components are parallel to the film plane. The curve of m_x versus H corresponds to the conventional hysteresis loop. In order to determine the PD of the FM layer, m_y was measured as a function of the orientation of the sample under a fixed H [18]. All measurements were performed at room temperature.

In experiments, we found that for the NiFe/FeMn bilayers, m_y is always zero when the hysteresis loop is measured along the deposition field. Therefore, the principal axes of the uniaxial and unidirectional anisotropies are collinear [19]. This is because the intrinsic uniaxial anisotropy of the magnetically soft NiFe layer is negligible, and thus the uniaxial anisotropy in the NiFe/FeMn bilayer is purely induced by the EB. Accordingly, we can define the deposition field direction as the initial PD along which the exchange bias initially acts. Any changes in the orientation of the PD can be monitored from the rotational variation of m_y in zero magnetic field; the PD can be identified as the angular position with $m_y = 0$ and a positive maximal m_x. The schematic picture for magnetic measurements is shown in the inset of Fig. 1, where θ_{PD} and $\theta_{H\text{-}Loop}$ represent, respectively, the orientations of the PD and H for measurements of hysteresis loops with respect to that of the initial PD. θ_{Rtn} is the angular variable for the rotational variation of m_y in zero magnetic field. For each sample, the initial PD was first identified from the rotational variation of m_y in zero magnetic field before the application of any external magnetic field. At a specific $\theta_{H\text{-}Loop}$, the hysteresis loop was measured and H_E and H_C were determined at $n = 1$. Afterwards, θ_{PD} was determined at $n = 1$ using the rotational variation of m_y in zero magnetic field. The above procedures were then repeated so that the variations of H_E, H_C, and θ_{PD} with n were acquired.

Figure 1(a) shows that for the uniform NiFe(3 nm)/FeMn(2.4 nm) bilayer at $\theta_{H\text{-}Loop} = -12$ degrees, the coercive field of the descending branch decreases significantly with increasing n while that of the ascending branch changes little. As shown in Fig. 1(b), m_y at the descending branch is increased after subsequent measurements, and the asymmetry of the hysteresis loop becomes weak. Figure 1(c) shows that θ_{PD} is shifted towards high angles after subsequent measurements. Apparently, the PD rotation has for the first time been probed directly during consecutive hysteresis loops. It is noted that similar phenomenon has been observed in FM/AFM bilayers in rotating magnetic fields [15]. As a new physical quantity, the quantitative estimation of the PD rotation is of crucial importance to the investigations of the EB training effect.

Figure 2 shows the variations of $H_E(n)$, $H_C(n)$, and $\theta_{PD}(n)$ with n at $\theta_{H\text{-}Loop} = -12$ degrees. It is interesting to note that the initial sharp decrease of $H_E(n)$ and $H_C(n)$ and a sharp increase of $\theta_{PD}(n)$ occur simultaneously. With increasing n, $H_E(n)$ and $H_C(n)$ decrease while $\theta_{PD}(n)$ increases. Alternatively, we can interpret the data as follows. As the angle between H and the rotated PD, i.e., $\theta_{PD}(n) - \theta_{H\text{-}Loop}$ increases, $H_E(n)$ and $H_C(n)$ decrease, which is consistent with the conventional angular dependence of the EB [20]. The rotation of the PD is at least one important contribution to the reductions of $H_E(n)$ and

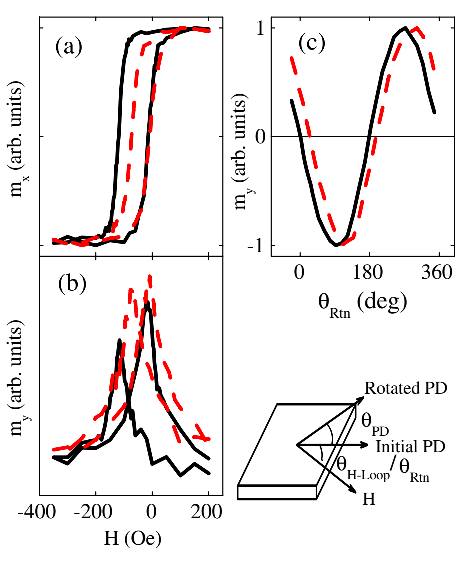

FIG. 1 (color online). Hysteresis loops m_x (a) and m_y (b) with $\theta_{H\text{-}Loop} = -12$ degrees, and the curves of m_y versus θ_{Rtn} in $H = 0$ (c) for the uniform NiFe(3 nm)/FeMn (2.4 nm) bilayer. In (a) and (b), $n = 1$ (black, solid line), 20 (red, dashed line). In (c), $n = 0$ (black, solid line), 20 (red, dashed line). The inset shows the schematic picture of magnetic measurements.

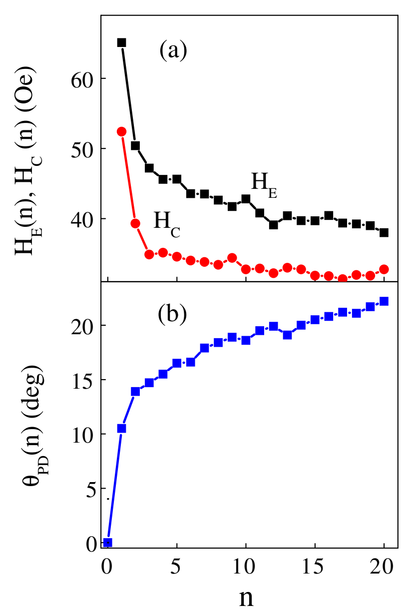

FIG. 2 (color online). Dependence of H_E and H_C (a) and θ_{PD} (b) on n for the uniform NiFe(3 nm)/FeMn (2.4 nm) bilayer, where consecutive hysteresis loops were measured at $\theta_{H\text{-}Loop} = -12$ degrees.

$H_C(n)$ in the training effect. Thus, in addition to the magnitude reduction of the exchange anisotropy [7], the PD rotation should also be considered in explanations of the EB training effect. For all nonzero values of $\theta_{\text{H-Loop}}$, we obtain similar results to those in Figs. 1 and 2.

Here, we use $\frac{\Delta H_{E/C}}{H_{E/C}(n=1)}$ and $\Delta\theta_{PD}$ to express, respectively, the relative changes of H_E and H_C and the orientation change of the PD, where $\Delta H_{E/C} = H_{E/C}(n=1) - H_{E/C}(n=20)$ and $\Delta\theta_{PD} = \theta_{PD}(n=20) - \theta_{PD}(n=0)$. Figures 3(a) and 3(b) show the angular dependence of $\frac{\Delta H_{E/C}}{H_{E/C}(n=1)}$ and $\Delta\theta_{PD}$ for the uniform NiFe(3 nm)/FeMn(2.4 nm) bilayer. At $\theta_{\text{H-Loop}} = 0$, $\Delta\theta_{PD} = 0$ while $\frac{\Delta H_E}{H_E(n=1)}$ and $\frac{\Delta H_C}{H_C(n=1)}$ still exist. At small negative $\theta_{\text{H-Loop}}$, $\Delta\theta_{PD}$ increases sharply and reaches a maximum while $\frac{\Delta H_E}{H_E(n=1)}$ and $\frac{\Delta H_C}{H_C(n=1)}$ change little. At large negative $\theta_{\text{H-Loop}}$, $\frac{\Delta H_E}{H_E(n=1)}$, $\frac{\Delta H_C}{H_C(n=1)}$, and $\Delta\theta_{PD}$ all decrease. Finally, near $\theta_{\text{H-Loop}} = -90$ degrees, $\Delta\theta_{PD}$ and $\frac{\Delta H_C}{H_C(n=1)}$ are close to zero. However, $\frac{\Delta H_E}{H_E(n=1)}$ increases because the denominator $H_E(n=1)$ is close to zero.

For the present NiFe/FeMn bilayer, the hysteresis loop asymmetry is similar in the angular dependence to $\Delta\theta_{PD}$. For simplicity, consider the $n = 1$ hysteresis loop as an example. In experiments, we found that at $\theta_{\text{H-Loop}} = 0$, m_y at the coercive field of either branch always equals zero and the asymmetry disappears. At small negative $\theta_{\text{H-Loop}}$, m_y is nonzero, and the asymmetry is prominent [6,10,11,21–23], as shown in Fig. 1(b). At large negative $\theta_{\text{H-Loop}}$, the asymmetry approaches zero again. In general, nonzero values of m_y indicate the presence of a component of rotation in the magnetization reversal mechanism; $m_y = 0$ corresponds to dominant domain wall motion. Apparently, $\Delta\theta_{PD}$, the asymmetry, and the magnetization reversal mechanism are correlated. The dramatic angular dependence of $\Delta\theta_{PD}$ is important evidence relating the PD rotation to the magnetization reversal mechanism of the FM layer.

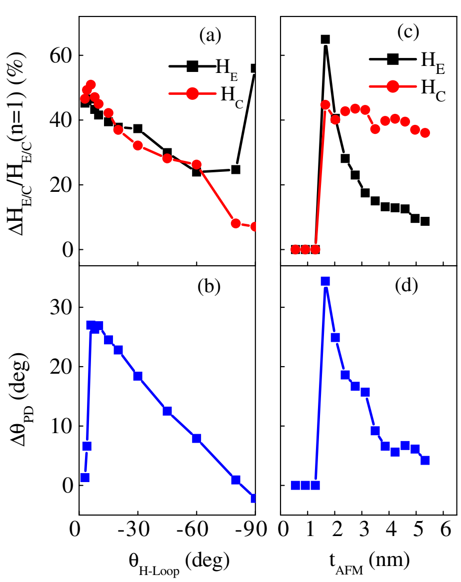

FIG. 3 (color online). Dependence of $\frac{\Delta H_E}{H_E(n=1)}$ and $\frac{\Delta H_C}{H_C(n=1)}$ (a), (c) and $\Delta\theta_{PD}$ (b), (d) on $\theta_{\text{H-Loop}}$ for the uniform NiFe(3 nm)/FeMn (2.4 nm) bilayer (a), (b) and on t_{AFM} at $\theta_{\text{H-Loop}} = -12$ degrees for NiFe(3 nm)/wedged-FeMn (0–6 nm) bilayers (c), (d).

The variation of $\Delta\theta_{PD}$ with $\theta_{\text{H-Loop}}$ can be understood using the thermal activation model [17,24]. For the interfacial uncompensated magnetic moment of an individual AFM grain, m_{AFM}, which is controlled by the interfacial roughness and is parallel to spins of one sublattice, the motion mode depends on the magnetization reversal mechanism of the FM layer due to the exchange field from the FM layer [25]. With domain rotation, m_{AFM} is irreversibly rotated by the rotating exchange field whereas it can only switch by 180 degrees due to switching of the exchange field with domain wall motion. Meanwhile, the probability of rotation or switching of m_{AFM} is controlled by both the thermal energy and the energy barrier. For the average uncompensated magnetic moment per unit area, $m_{\text{AFM-AVE}}$, both the magnitude [26] and the orientation might change. Since the PD orientation is determined by that of $m_{\text{AFM-AVE}}$ [27], the PD may be rotated during the EB training. Apparently, at $\theta_{\text{H-Loop}} = 0$, with domain wall motion, the orientation of $m_{\text{AFM-AVE}}$ is still aligned along that of the initial PD, resulting in $\Delta\theta_{PD} = 0$ as shown in Fig. 3(b). At small negative $\theta_{\text{H-Loop}}$, the fraction of the domain rotation is different for two branches of the hysteresis loop, as revealed by the prominent asymmetry in Fig. 1(b). Hence, the change in the orientation of $m_{\text{AFM-AVE}}$ is different for the two branches, resulting in a large $\Delta\theta_{PD}$. At large negative $\theta_{\text{H-Loop}}$, the fraction of the domain rotation is similar for the two branches, as demonstrated by a weak asymmetry [21]. In this case, the irreversible rotations of $m_{\text{AFM-AVE}}$ in two branches tend to cancel so that $\Delta\theta_{PD}$ is reduced. Hence, the nonmonotonic variation of $\Delta\theta_{PD}$ with $\theta_{\text{H-Loop}}$ indicates that the motion of $m_{\text{AFM-AVE}}$ in the EB training effect depends on the magnetization reversal mechanism of the FM layer.

Figures 3(c) and 3(d) show the dependence of $\frac{\Delta H_{E/C}}{H_{E/C}(n=1)}$ and $\Delta\theta_{PD}$ on t_{AFM} for NiFe(3 nm)/FeMn bilayers at $\theta_{\text{H-Loop}} = -12$ degrees. $\frac{\Delta H_E}{H_E(n=1)}$, $\frac{\Delta H_C}{H_C(n=1)}$, and $\Delta\theta_{PD}$ are equal to zero at small t_{AFM} and then increase to reach maxima with increasing t_{AFM}. Finally, they decrease with further increasing t_{AFM}. These results can also be explained in terms of the thermal activation model [24]. The transition probability of AFM spins, and m_{AFM} is assumed to be governed by the competition between the thermal energy and the energy barrier. The latter one is proportional to t_{AFM}, assuming the lateral area of grains is fixed. With small t_{AFM}, AFM spins in most grains are ‘‘superparamagnetic’’ and thus the training effect and the PD deviation

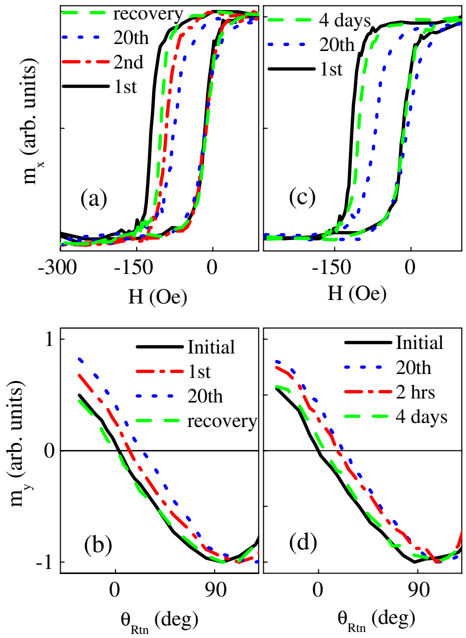

FIG. 4 (color online). Hysteresis loops at $\theta_{\text{H-Loop}} = -12$ degrees (a), (c) and angular dependence of m_y under $H = 0$ (b), (d) using the first (a), (b) and the second (c), (d) recovery methods for the uniform NiFe(3 nm)/FeMn (2.4 nm) bilayer.

vanish [17,24]. With increasing t_{AFM}, AFM spins in most of AFM grains are thermally stable [28]. Since AFM spins can be rotated irreversibly, the PD deviation reaches a maximum, so does the training effect. As t_{AFM} is further increased, the volume of AFM grains and accordingly the anisotropy energy barrier increase, resulting in a reduction in probability of thermally activated transitions. The PD deviation and the training effect are suppressed.

Although the EB recovery has been studied more recently [9], direct observation of the PD can further elucidate the nature of this phenomenon. Here, we study the EB recovery in the uniform NiFe(3 nm)/FeMn (2.4 nm) bilayer. Initially, $n = 20$ hysteresis cycles were measured at $\theta_{\text{H-Loop}} = -12$ degrees. Afterwards, the EB recovery was performed by one of the following two methods. In the first approach, one hysteresis loop was measured at $\theta_{\text{H-Loop}} = 78$ degrees [9]. In the second approach, H was set to zero for a designated period. Finally, the rotational variation of m_y in zero magnetic field and the hysteresis loop at $\theta_{\text{H-Loop}} = -12$ degrees were recorded in turn. Figures 4(a) and 4(c) show that with either approach, H_E and H_C are increased after the recovery procedure, compared with those of $n = 20$. Meanwhile, the PD approaches the initial one, as shown in Figs. 4(b) and 4(d). Therefore, the variation of θ_{PD} *directly* verifies the theoretical prediction that $m_{\text{AFM-AVE}}$ and AFM spins are also rotated during the EB recovery [9].

In summary, the PD in polycrystalline FM/AFM bilayers has been found to deviate from and approach the initial PD in the EB training and recovery effects, respectively. The nonmonotonic variation of $\Delta\theta_{\text{PD}}$ with $\theta_{\text{H-Loop}}$ suggests that the orientation change of $m_{\text{AFM-AVE}}$ depends on the magnetization reversal mechanism of the FM layer. m_{AFM} may acquire 180-degree switching and rotation in the cases of domain wall motion and domain rotation in the FM layer, respectively. $\Delta\theta_{\text{PD}}$ also depends on t_{AFM}. These results can be explained in terms of the thermal activation model. The present work uncovers the general picture of the motion of AFM spins in the EB training effect [12,13].

This work was supported by the National Science Foundation of China under Grant Nos. 50625102, 10574026, and 60490290; the National Basic Research Program of China under Grant Nos. 2007CB925104 and 2009CB929201; 973-project under Grant No. 2006CB921300; Shanghai Science and Technology Committee under Grant No. 06DJ14007; and Shanghai Leading Academic Discipline Project under Grant No. B113.

[1] See, e. g., J. Nogués and I. K. Schuller, J. Magn. Magn. Mater. **192**, 203 (1999).
[2] A. E. Berkowitz and K. Takano, J. Magn. Magn. Mater. **200**, 552 (1999).
[3] K. Zhang *et al.*, J. Appl. Phys. **89**, 6910 (2001).
[4] D. Suess *et al.*, Phys. Rev. B **67**, 054419 (2003).
[5] F. Radu *et al.*, Phys. Rev. B **67**, 134409 (2003).
[6] A. Hoffmann, Phys. Rev. Lett. **93**, 097203 (2004).
[7] C. Binek, Phys. Rev. B **70**, 014421 (2004).
[8] T. Hauet *et al.*, Phys. Rev. Lett. **96**, 067207 (2006).
[9] S. Brems *et al.*, Phys. Rev. Lett. **95**, 157202 (2005); **99**, 067201 (2007).
[10] E. Pina *et al.*, Phys. Rev. B **69**, 052402 (2004).
[11] T. Gredig *et al.*, Phys. Rev. B **74**, 094431 (2006).
[12] H. W. Xi *et al.*, Phys. Rev. B **64**, 184416 (2001).
[13] S. Polisetty *et al.*, Phys. Rev. B **76**, 184423 (2007).
[14] B. H. Miller and E. Dan Dahlberg, Appl. Phys. Lett. **69**, 3932 (1996).
[15] T. Gredig *et al.*, J. Appl. Phys. **87**, 6418 (2000).
[16] R. Nakatani, Jpn. J. Appl. Phys. **33**, 133 (1994).
[17] T. R. Gao *et al.*, Phys. Rev. Lett. **99**, 057201 (2007).
[18] L. Benito *et al.*, Rev. Sci. Instrum. **77**, 025101 (2006).
[19] T. Pokhil *et al.*, J. Magn. Magn. Mater. **272**, E849 (2004).
[20] H. Sang, Y. W. Du, and C. L. Chien, J. Appl. Phys. **85**, 4931 (1999).
[21] J. Camarero *et al.*, Phys. Rev. Lett. **95**, 057204 (2005).
[22] D. Spenato *et al.*, Appl. Phys. Lett. **91**, 062515 (2007).
[23] M. S. Lund and C. Leighton, Phys. Rev. B **76**, 104433 (2007).
[24] D. Choo *et al.*, J. Appl. Phys. **101**, 09E521 (2007).
[25] B. Beckmann *et al.*, Phys. Rev. Lett. **91**, 187201 (2003).
[26] A. Hochstrat *et al.*, Phys. Rev. B **66**, 092409 (2002).
[27] H. W. Xi *et al.*, Appl. Phys. Lett. **74**, 2687 (1999).
[28] M. D. Stiles and R. D. McMichael, Phys. Rev. B **59**, 3722 (1999).